Fluorescence Dynamics of Double- and Single-Stranded DNA Bound to Histone and Micellar Surfaces

Teena Goel,[†] Tulsi Mukherjee,[†] Basuthkar J. Rao,*[,‡] and Guruswamy Krishnamoorthy*[,§]

Radiation and PhotoChemistry Divison, Chemistry Group, Bhabha Atomic Research Center, Mumbai 400 085, India, and Departments of Biological Science and Chemical Science, Tata Institute of Fundamental Research, Homi Bhabha Road, Mumbai 400 005, India

Received: December 21, 2009; Revised Manuscript Received: June 7, 2010

The study of structure and dynamics of bound DNA has special implications in the context of its biological as well as material functions. It is of fundamental importance to understand how a binding surface affects different positions of DNA with respect to its open ends. Because double-stranded (ds) and single-stranded (ss) DNA are the predominant functional forms, we studied the site-specific dynamics of these DNA forms, bound to the oppositely charged surface of histones, and compared the effects with that of DNA bound to cetyltrimethyl ammonium bromide micelles. We utilized a time-resolved fluorescence technique using fluorescent base analogue 2-aminopurine located at specific positions of synthetic poly-A DNA strands to obtain fluorescence lifetime and anisotropy information. It is observed that the binding leads to overall rigidification of the DNA backbone, and the highly flexible ends show drastic dampening of their internal dynamics as well as the fraying motions. In the case of ds-DNA, we find that the binding not only decreases the flexibility but also leads to significant weakening of base-stacking interactions. An important revelation that strong binding between DNA and the binding agents (histones as well as micelles) does not dampen the internal dynamics of the bases completely suggests that the DNA in its bound form stays in some semiactive state, retaining its full biological activity. Considering that the two binding agents (histones and micelles) are chemically very different, an interesting comparison is made between DNA−histones and DNA−micelle interactions.

1. Introduction

Understanding the structure and dynamics of condensed (or bound) DNA has been a subject of current interest due to its relevance in natural conditions like DNA packaging in chromosomes,[1] transcriptional regulation in chromatin,[2] and artificial systems like gene transfection..[3,4] Although the structural and dynamical aspects of DNA have largely been associated with its sequence,[5,6] the influence of the contact with the surfaces is also expected to have a phenomenal effect on the conformation and the dynamics of large biomolecules.[7] There have been extensive studies on structural aspects of DNA condensed with various condensing agents such as cationic lipids,[8,9] surfactants,[10,11] and peptides,[12] but only limited information is available on their dynamical aspects. The extent and the position of interaction of the complexing agents with DNA are reflected in the segmental and internal dynamics of DNA.

In eukaryotic cells, DNA exists in a highly condensed form, supercoiled and wound on basic proteins called histones[13,14] in a structure, which is collectively labeled as chromatin. Several post-translational modifications in histones in the form of methylation, phosphorylation, or acetylation affect the net charge, shape, and other properties of histones, as well as the structural and functional properties of the chromatin. The presence and the level of single-stranded breaks and the extent of rigidity of DNA while bound to histones are important issues related to the level of DNA integrity in chromosomes. Binding with the oppositely charged surface provides DNA with more structural stability, protection against nucleases,[15] and destabilization effects at high temperature[16] or other drastic changes occurring in the surrounding, while retaining its full functional stability, besides conferring a general repressive effect on transcription.[17]

To understand the dynamics of DNA in the bound state, we have employed positively charged cetyl trimethyl ammonium bromide (CTAB) micelles ($\leq$30 Å diameter, aggregation number $\approx$60 at room temperature[18]) as a model binding agent. CTAB is one of the most widely used condensing agents for DNA, and the structure along with the phase behavior of the DNA−CTAB complex is well-characterized through NMR relaxation, light scattering techniques, circular dichroism (CD), and simulation methods.[8,9,19–23] CTAB is used to extract DNA from protein−DNA solutions and is also used as a vector to transport DNA through various membranes in cells used in gene therapy experiments.[24] The dynamics of DNA is observed to be restricted after condensation with polyethylenimine (PEI), CTAB surfactant, and inorganic complexing agents.[10] It is understood that the positively charged surface of CTAB micelles interacts with the negatively charged DNA backbone initially through electrostatic interactions later enhanced cooperatively by the hydrophobic interactions between their backbones.[25]

The dynamics of DNA in nucleosome core particles and in the linker region of chromatin has been previously studied using nanosecond fluorescence anisotropy decay measurements of intercalated DNA using ethidium bromide as the fluorophore.[26–32]

* To whom correspondence should be addressed. Tel: +91 22 2278 2301 or +91 98921 00404. Fax: +91 22 2280 4610. E-mail: bjrao@tifr.res.in (B.J.R.) or gk@tifr.res.in (G.K.).

[†] Bhabha Atomic Research Center.

[‡] Department of Biological Science, Tata Institute of Fundamental Research.

[§] Department of Chemical Science, Tata Institute of Fundamental Research.

10.1021/jp912029m
Published on Web 06/22/2010

TABLE 1: Samples Used in the Present Work[a]

	Sample	
1.	A30(*):T30	1st 2nd 15th 5'A*A*AAAAAAAA[10]AAAAA*AAAAA[20]AAAAAAAAAA3' 5' TTTTTTTTTT[10]TTTTTTTTTT[20]TTTTTTTTTT 3'
2.	A30(*)	1st 2nd 15th 5'A*A*AAAAAAAA[10]AAAAA*AAAAA[20]AAAAAAAAAA3'

[a] A* ≡ 2-AP.

A time-resolved triplet state anisotropy decay technique has been used to measure the conformational flexibility of DNA in the nucleosome.[28] To date, no detailed study has been done exploring the effect of binding agents on dynamics of specific positions of DNA with respect to the ends. This information has significant potential to give clues about why some positions in DNA strand are more prone to nuclease attack or show specific binding affinities for various proteins. The position of the nucleotide sequence with respect to the open ends has important implications on the function of DNA.[33–38]

In the present work, we have studied the position-dependent dynamics of double-stranded (ds) and single-stranded (ss) DNA in free form and bound to agents such as histones and CTAB micelles through a time-resolved fluorescence technique. We have chosen synthetic oligonucleotides that are comprised of repeats of adenine. We deliberately avoided mixed sequences so as to ensure that any observed effect is due to its position dependence instead of base identity. We used the fluorescent analogue of adenine, 2-aminopurine (2-AP), as a probe located at different positions of DNA strands with respect to the ends. 2-AP has been extensively used as an indicator of conformational and environmental changes of DNA as its fluorescence intensity is quite sensitive to local dynamics of bases, stacking, and base-pairing interactions.[39–44] An earlier work described the intricacies of site-specific dynamics of strands in ss- and ds-DNA using fluorescence decay kinetic measurements.[45] In this work, 2-AP was located as one of the bases in synthetic DNA strands to obtain dynamical information of various positions of ss-DNA and ds-DNA with respect to the ends. The fluorescence lifetime and anisotropy decay kinetics provide direct information on various modes of dynamics in biopolymers such as local (internal) dynamics, segmental dynamics of the polymer backbone, and the global tumbling motion of the entire macromolecule.[46–51] The unexpected dependence of the motional dynamics of the bases and DNA backbone on the position with respect to the ends of DNA has been our motivation to further understand the effect of external binding agents on dynamics of specific positions of DNA strands. Our results show qualitative and quantitative aspects of dynamics of free and bound ss- and ds-DNA. Interesting similarities have been observed between two model systems (histones and CTAB), although the binding agents possess different chemical and physical properties. The results are discussed keeping DNA functions in perspective.

2. Materials and Methods

2.1. Materials. The single-stranded oligonucleotides with a 2-AP fluorescent base analogue at different positions of the strand were obtained from DNA Technology (Aarhus, Denmark). The crude oligonucleotides were purified using PAGE (polyacrylamide gel electrophoresis) chromatography, the procedure as described earlier.[52] The concentration of stock DNA sample was measured through absorption at 260 nm and expressed as total nucleotide concentration. The different oligomers used for the present study are described in Table 1. The nomenclature of the samples is, for example, A30(1)T30, and refers to the annealed product of a 1:1 mixture of A-30mer and T-30mer with 2-AP placed at the first position from the 5′-end of the poly-A strand. CTAB, 99.9% pure, was purchased from Sigma Chemical Co. All of the solutions were prepared using deionized (Millipore), autoclaved water. A lyophilized sample of calf thymus core histones H4 was obtained from Roche Chemicals.

2.2. Sample Preparation. Duplex DNA was prepared by annealing ss-oligomers, done by mixing the labeled strand (0.5 mM A-30mer) with its complementary unlabeled strand (0.5 mM T-30mer) in a total volume of 50 μL followed by heating at 85 °C for 2 min in 10 mM Tris Cl (pH 7.5) and 10 mM Mg-Acetate and slow cooling to the room temperature (~25 °C) over a period of 45 min. The ratio of the concentration of the two strands was 1:1. Completion of annealing was assessed by autoradiographic analyses of an aliquot on 10% native polyacrylamide gel, which showed that more than 90% labeled strand was converted to duplexes and no residual, unannealed, labeled ss-DNA was present.[53–55] The concentration of DNA was expressed as nucleotide concentration. The final solution containing a 20 μM nucleotide concentration of DNA bases in 20 mM HEPES buffer (pH 7.4) was used for all of the fluorescence measurements. The possibility of triplex (TAT) formation during the sample preparation was ruled out based on the fluorescence lifetime data. The mean lifetime value of the 2-AP located on ss-DNA and on triplex shows a larger value as compared to that of duplexes.[56] In the present case, the mean lifetime value of the (1:1) sample was observed to be the lowest as found from titrations of the two strands, thus confirming the formation of duplex without a significant population of either ss-DNA or triplexes.

A 0.1 mg sample of H4 histones was dissolved in 500 μL of buffer solution consisting of 20 mM sodium phosphate, 300 mM sodium chloride, 1 mM dithiothreitol (DTT), and 1 mM ethylene diaminetetraacetic acid (EDTA) keeping the pH at 7.0 to make the stock concentrate. The histone sample was then stored at −20 °C and divided into 10 aliquots. During each set of measurements, ~10 μM histones was added to ~20 μM nucleotide concentration of DNA bases.

The concentration of the stock CTAB micellar solution was taken as 100 mM, which was diluted to 2 mM (twice its critical micellar concentration ≈0.9 mM) while adding to the final DNA sample mixture. The aggregation number of CTAB micelles

was ~60 at 2 mM concentration, and the average micellar diameter corresponded to ~30 Å. The background fluorescent impurity of CTAB solution was found to be less than 5% of total fluorescence of the sample and thus lies within the accepted error limits. Measurements were done at room temperature (22 ± 1 °C). It must be noted that the critical micelle concentration (CMC) of CTAB changes significantly only in the presence of a stoichiometric ratio of the DNA strands. In the present situation, the concentration of DNA was 20 μM nucleotides, which is quite negligible as compared to 2 mM surfactant concentration; hence, we do not expect the CMC of CTAB to change significantly. Furthermore, the concentration of CTAB (2 mM) used was much above the CMC (≈0.9 mM) so that there was a very low probability of the presence of individual surfactant molecules.

2.3. Fluorescence Measurements. Steady-state fluorescence spectra were recorded using a SPEX Fluorolog FL 111 T-format spectrofluorimeter. The excitation source was a Xe lamp. All of the fluorescence spectra were corrected for the spectral sensitivity of the photomultiplier (Hamamatsu R928A). The bandwidth used was between 1 and 2 nm. Appropriate filters were used before the emission monochromator to avoid the excitation light entering it.

Time-resolved fluorescence measurements were done using a picosecond time-correlated single photon counting (TCSPC) technique.[57] The Rhodamine 6G dye laser pumped by CW passively mode-locked frequency-doubled Nd:YAG (Vanguard Spectra Physics, United States) was used as the excitation source, which generates 1 ps pulses of width. The excitation of 2-AP was done at 310 nm, which is the second harmonic output of an angle-tuned KDP crystal, and the emission was collected at 370 nm by a microchannel plate photomultiplier (model 2809u; Hamamatsu Corp.). The half-width of the instrument response function was ~40 ps. A 345 nm cutoff filter was used to prevent scattering of the excitation beam from the samples. The total collection at the peaks was at least 10000 counts.

Fluorescence lifetime measurements were done at the magic angle (54.7°) to eliminate the contribution from the anisotropy decay. Intensity decays were deconvoluted with the instrument response function and analyzed as a sum of exponentials,[58] that is,

$$I(t) = \sum \alpha_i \exp(-t/\tau_i) \tag{1}$$

where $I(t)$ is the fluorescence intensity at time t and τ_i is the individual lifetime with a corresponding amplitude α_i, such that $\sum\alpha_i = 1$. The mean lifetime $\tau_m = \sum_i \alpha_i\tau_i$, which is the area under $I(t)$ vs t curves, gave information on the average fluorescence yield of the system.

Time-resolved fluorescence anisotropy was calculated using the emission intensity parallel ($I_{||}$) and perpendicular ($I_\perp$) to the polarization of the excitation beam, according to the formula:

$$r(t) = \frac{I_{||}(t) - I_\perp(t)G(\lambda)}{I_{||}(t) + 2I_\perp(t)G(\lambda)} \tag{2}$$

where $G(\lambda)$ is the instrumental correction factor at the wavelength λ of emission and is the ratio of efficiency of detection for vertically and horizontally polarized light. The G factor of the emission collection optics was determined using a standard solution of 2-AP for which the fluorescence lifetime is ~11 ns. The anisotropy decays were analyzed by the following equations

$$I_{||}(t) = I(t)[1 + 2r(t)]/3$$

$$I_\perp(t) = I(t)[1 - r(t)]/3$$

$$r(t) = r_0\{\beta_1 \exp(-t/\varphi_1) + \beta_2 \exp(-t/\varphi_2)\} \tag{3}$$

where r_0 is the initial anisotropy and β_i is the amplitude of the i-th rotational correlation time ϕ_i such that $\sum_i\beta_i = 1$. These parameters were obtained by deconvoluting the decays with IRF, and the initial anisotropy, r_0, estimated in a separate experiment on 2-AP in 50% glycerol, was kept fixed during the analysis. During analysis, the values of α_i and τ_i were kept fixed to reduce the number of floating parameters. The goodness of fits were checked by both the reduced χ^2 value and randomness of residuals.

The values of lifetimes and rotational correlation times obtained for several samples were in the range of 0.1−0.3 ns. As these values were quite close to both the width of the instrument response function and the time/channel used, both of which were ~40 ps, their reliability might seem uncertain. To check the reliability of such measurements, we measured the rotational correlation time (Φ) of a small molecule *N*-acetyltryptophanamide (NATA) in glycerol−water mixtures with a viscosity (η) in the range of 1−5 cP. The values of Φ estimated were 0.063 ± 0.023, 0.121 ± 0.033, 0.228 ± 0.026, and 0.315 ± 0.025 ns when the solvent viscosities were 1.0, 2.1, 4.4, and 5.4 cP, respectively, as expected from the Stokes−Einstein relationship ($\Phi = \eta V/kT$, where V is the molecular volume).

2.4. Fluorescence Quenching Measurements. The fluorescence intensity (I) and fluorescence lifetime (τ) of 2-AP-labeled oligomers with and without CTAB micelles were measured using increasing concentrations of acrylamide. The collisional quenching of fluorescence in each case showed a linear dependence on the concentration of the quencher, and the data are analyzed by fitting to the Stern−Volmer equation[47]

$$\tau_0/\tau = 1 + K_{SV}[Q] \tag{4}$$

where τ_0 and τ are the fluorescence lifetimes in the absence and presence of the quencher, respectively, $[Q]$ is the molar concentration of the quencher, and K_{SV} is the Stern−Volmer quenching constant, which is equal to $k_q\tau_0$, where k_q is the bimolecular quenching rate constant (M^{-1} s^{-1}) and τ_0 is the fluorophore lifetime in the absence of the quencher.

3. Results and Discussions

In this work, we present insights into site-specific dynamics of bound DNA. We have chosen site-specific fluorescence-labeled ds- and ss-DNA and studied picosecond time-resolved fluorescence emission analyses to understand stacking interactions, solvent accessibility, and motional dynamics of DNA in free and bound states. To avoid sequence context-based effects, we used DNA with repeat units, in this case oligo A (adenine) and T (thymine) repeat strands (Table 1). The oligo-A repeat chain with a fluorescent base analog, 2-AP, incorporated at varying locations with respect to the end has been used. To understand the effect of histones on the structure and dynamics of DNA, we have studied one of the core histones (H4) and analyzed the time-resolved fluorescence decay kinetics of 2-AP associated with the H4−DNA complex. Among all of the core histones, H4 is the smallest [molecular weight (MW) = 11236 Da, net positive charge on histone = 18].[13] CTAB micelles with

TABLE 2: Parameters Associated with Fluorescence Intensity Decay and Fluorescence Anisotropy Decay in ds-DNA in the Presence of Histone H4 and CTAB Micelles[a]

	fluorescence lifetime (ns) (amplitude)				mean lifetime (ns)	% inc. in	rotational correlation time (ns) (amplitude)	
sample	τ_1 (α_1)	τ_2 (α_2)	τ_3 (α_3)	τ_4 (α_4)	τ_m	τ_m	ϕ_1 (β_1)	ϕ_2 (β_2)
A30(1)T30	0.18 (0.37)	0.76 (0.32)	1.8 (0.24)	5.3 (0.07)	1.13		0.19 (0.27)	3.2 (0.73)
A30(2)T30	0.07 (0.58)	0.47 (0.17)	1.6 (0.19)	6.8 (0.06)	0.85		0.37 (0.29)	5.1 (0.71)
A30(15)T30	0.06 (0.66)	0.22 (0.27)	1.6 (0.04)	7.5 (0.03)	0.40		0.63 (0.59)	13.4 (0.41)
A30(1)T30 + H4	0.14 (0.31)	0.90 (0.26)	3.0 (0.25)	7.9 (0.18)	2.48	118	0.76 (0.22)	40 ± 5 (0.78)
A30(2)T30 + H4	0.08 (0.33)	0.44 (0.21)	1.9 (0.25)	7.0 (0.21)	2.08	144	0.70 (0.11)	75 ± 15 (0.89)
A30(15)T30 + H4	0.08 (0.58)	0.94 (0.29)	1.9 (0.08)	7.6 (0.07)	0.76	90	0.68 (0.21)	>100 (0.79)
A30(1)T30 + CTAB	0.13 (0.32)	0.73 (0.31)	2.3 (0.26)	6.2 (0.11)	1.52	34	0.65 (0.42)	15.6 (0.58)
A30(2)T30 + CTAB	0.08 (0.37)	0.51 (0.27)	2.0 (0.24)	6.2 (0.12)	1.37	60	0.58 (0.36)	23 (0.64)
A30(15)T30 + CTAB	0.09 (0.60)	0.44 (0.19)	1.8 (0.14)	5.5 (0.07)	0.79	96	0.66 (0.35)	25 (0.65)

[a] Note that the error associated with the estimation of τ_1 is ~20%, and those of τ_2 and τ_3 are ~10%, whereas the error in τ_m estimation is ~5%. The significantly lower value of error associated with τ_m is due to compensation of the larger uncertainties associated with the individual components. The error in ϕ_1 estimation is ~20%, and that with ϕ_2 is ~15% unless otherwise mentioned. Individual values of errors are not given to reduce the clutter.

positive-charged surfaces provide the simplest and convenient artificial model to extend the analogy with histone molecules. Micelle−DNA interactions have been well-studied in different aspects of DNA conformations, packing of micellar structures, and effects of binding to the micellar surface on the stability and vulnerability of DNA toward external agents such as nucleases, etc.[15,16,19–23] In this study, we focus on the comparison of the dynamics of various positions with respect to the ends of ds-DNA and ss-DNA in the presence of external binding agents. The time-resolved fluorescence intensity and anisotropy data of 2-AP provide both quantitative and qualitative aspects of dynamics of bound and free DNA. We compare and contrast between the influence of two binding agents, one natural (histones) and the other artificial (CTAB micelles), using synthetic strands of ds- and ss-DNA.

3.1. Interaction of Double-Stranded DNA (A30-T30) with H4 Histones and CTAB.

3.1.1. Fluorescence Lifetime Analysis. The fluorescence lifetime of 2-AP located in ds-DNA is mainly controlled by local internal motion and stacking interactions and accessibility to the solvent. Free 2-AP in solution has a fluorescence quantum yield of 0.68 at pH 7[44] and has a single lifetime of 11.6 ns. The fluorescence of 2-AP is strongly quenched when incorporated in DNA, and the level of quenching is sensitive to local and global changes in DNA conformations.[40,41,44] When incorporated into an oligonucleotide, 2-AP shows heterogeneous fluorescence decay with time constants ranging from ~50 ps to ~10 ns.[40,41,44–46,56,59,60] This is interpreted as due to the distribution of partially stacked structures with varying dynamics. The heterogeneity in the DNA population observed through fluorescence lifetimes is not seen from other measurements such as NMR, CD, etc., probably due to averaging of various conformers. The rapid time scale associated with fluorescence decay kinetics enables the visualization of various conformers as a snapshot picture. We studied the interactions of A30-T30 ds-DNA having 2-AP located at 1st, 2nd, and 15th positions (Table 1) on the poly-A strand with H4 histone. The fluorescence intensity decay curves have been satisfactorily fitted to a sum of four exponentials, and the mean lifetime values along with their individual lifetime components are shown in Table 2. These four lifetime components originate from four different conformational dynamics of 2-AP in ds-DNA.

The fastest lifetime component ($\tau_1 \sim 0.05-0.2$ ns) could be considered as a signature of base-pair formation[45,46,56,61] in ds-DNA. Stronger base-pair formation is associated with a stronger stacking interaction of 2-AP with near neighbor bases leading to a shorter value of τ_1 and a larger value of the amplitude α_1 associated with this lifetime component.[45,46,61] The larger value of τ_1 when 2-AP is placed at the end of the duplex as compared to its middle position is consistent with the weaker level of stacking interactions at the end of the duplex. The longest component (5−8 ns) is assigned to conformations where the 2-AP is either extrahelical or unstacked in the DNA. The amplitude of the longest component (α_4) is significantly smaller as compared to the amplitude of fastest component (α_1), which indicates that the dominant conformation of 2-AP in ds-DNA is characterized by stacking between the bases. The mean lifetime value of the probe, τ_m, increases substantially (~90−140%, Table 2, rows 4−6), irrespective of its position on the ds-DNA strand when it binds to the histone. This is expected as binding imposes restrictions in the local movements of the bases and thus causes reduction in nonradiative decay of the fluorophore. The value of τ_m decreases as the probe position changes with respect to the ends in bound ds-DNA, which is similar in trend as that of free ds-DNA, indicating that the site specificity of dynamics is preserved on binding to the external surfaces. One interesting observation is that the amplitude (α_1) of the shortest lifetime component (τ_1) decreases for all of the probe positions on binding to the histones. It implies that stacking interactions between bases (and probably base-pairing interactions) becomes weaker when ds-DNA binds to the histone. To see whether this effect is a general phenomenon in the presence of any external binding agent, we checked the fluorescence decay components of ds-DNA in the presence of CTAB micelles and found consistency in this observation (Table 2, rows 7−9). An interesting correlation of the above information can be made with the fact that binding of some proteins leads to easy unwinding of DNA strands in a duplex since binding leads to weakening of stacking and base-pairing interactions. It is worth noticing that the extent of weakening in these interactions is more with the histones than with CTAB micelles, as is evident from the lesser value of α_1 in the case of histones than in micelles. This shows that histones are more efficient binders to DNA than micelles.

The mean lifetime (τ_m) of the probe located on ds-DNA bound to the micelle shows a similar trend in site specificity as that of histone-bound ds-DNA. The concentration of micelles in DNA solution is taken sufficiently high to ensure that all probed DNA strands bind to at least one micelle. We checked the binding of DNA with higher concentrations of CTAB micelles and found no further increase in lifetime of the probe, indicating that all of the bound probes are saturated at a 2 mM micellar concentration. The interaction of the positively charged CTAB micelles and negatively charged DNA backbone is reported

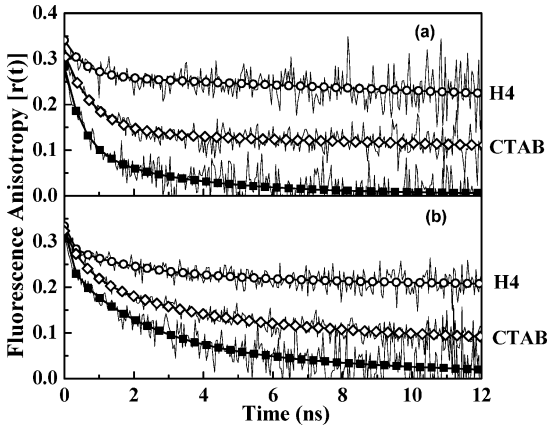

Figure 1. Fluorescence anisotropy decay plots of 2-AP located in A30-T30 ds-DNA at (a) position 15 and (b) position 1, in free form and condensed form with core histone H4 and CTAB micelles. Filled squares, control; diamonds, CTAB; and open square, H4 histone.

mainly as electrostatic interactions complemented by hydrophobic forces.[25]

3.1.2. Time-Resolved Fluorescence Anisotropy. Fluorescence anisotropy decay curves for 2-AP located on ds-DNA bound to H4 histones were satisfactorily fitted to a sum of two exponentials (values shown in Table 2), and typical traces of anisotropy decay for free and bound ds-DNA are shown in Figure 1. The faster rotational correlation time (ϕ_1 or ϕ_{fast}) corresponds to the local motion of the probe with respect to the strand backbone such as propeller twist motion, bending and rocking motion, etc. The transition moment of 2-AP, which is nearly perpendicular to the long axis of DNA,[62] would undergo a change in its direction caused by these motional degrees of freedom, causing the observed rapid decay of fluorescence anisotropy decay. The slower rotational correlation time (ϕ_2 or ϕ_{slow}) has a combined contribution from both segmental dynamics of the nucleotide backbone and global tumbling of the entire DNA strand. Binding to an external agent such as histone has a strong effect on the dynamics of the nucleotides. The value of both correlation times (ϕ_1 and ϕ_2) of the probe increases in duplex bound to H4 histones as well to CTAB micelles. The increase in ϕ_1 value is expected due to imposition of restriction on the fraying motion of the ends on binding to the histones. The value of ϕ_1 is nearly the same for the probe located at all positions ($\sim$0.7−0.8 ns) of the histone-bound ds-DNA, suggesting that the internal dynamics of the probe is similar at all of the positions of the bound DNA. Moreover, it also shows that the dynamics of DNA strand is dampened but not completely restricted in the presence of the binding agents. The amplitude (β_1) associated with ϕ_1 increases from the end (0.27) to the middle (0.59) position of the probe located in the free ds-DNA strand, probably due to the concerted motion of stacked base pairs,[63] which becomes more probable at the interior of ds-DNA strands and recedes toward the ends.[45] When bound to either H4 histones or CTAB micelles, the amplitude (β_1) no longer shows an increasing trend toward the interior of the bound duplex (Table 2), suggesting that binding disrupts the correlated motion of bases in ds-DNA strands. There is a large increase in the value of the slower correlation time ϕ_2 as the position of the probe changes from end to the middle position of the bound duplex. The value of ϕ_2 exceeds the accuracy limit of detection measurements; thus, the values reported here represent the lower limit. ϕ_2 is >100 ns at the middle position of histone-bound ds-DNA. ϕ_2 represents a combination of the segmental dynamics around the probe and the global tumbling dynamics of ds-DNA. The former dynamics is faster than the latter. Hence, the increase in ϕ_2 value indicates a decreasing contribution of segmental dynamics when monitored at the middle of the bound ds-DNA strand. Such a large value of ϕ_2 (>100 ns) at the middle position of histone-bound ds-DNA should represent only global motion of the whole complex, as the time scale of segmental motion is very small as compared to the global motion. Moreover, such a large value of ϕ_2 also suggests an increased size of the histone−ds-DNA complex to which the probe is attached.

TABLE 3: Hydrodynamic Sizes of CTAB Micelles and H4 Histones and Their Complexes with ds- and ss-DNA Samples as Revealed by DLS Measurements

sample	hydrodynamic radius (nm)
2 mM CTAB micelles	4.0 ± 1
histone H4	34 ± 3
ds-DNA + H4	98 ± 10
ds-DNA + 2 mM CTAB	94 ± 9
ss-DNA + H4	56 ± 6
ss-DNA + 2 mM CTAB	88 ± 9

The qualitative behavior of changes in both the lifetime and the rotational correlation time is seen to be the same with both binding agents, that is, histones and CTAB micelles. Quantitatively, the effect of binding of ds-DNA to histones is observed to be more drastic than with CTAB micelles in terms of an increase in mean lifetime and rotational correlation time values for all of the positions, indicating more effective binding of ds-DNA with histones than CTAB micelles. The "% increase in τ_m" value of the probe (Table 2) is much higher when ds-DNA binds to the histones (in the range of $\sim$144−90%) as compared to the micellar binding (in the range of $\sim$30−90%). Similarly, the values of slower rotational correlation time (ϕ_2) are much higher in the case of histones (value >100 ns) than CTAB micelles (value $\sim$25 ns). A higher value of ϕ_2 suggests that the histone−ds-DNA complex is larger in size than the CTAB−ds-DNA complex. To check the sizes of the free and bound ds-DNA, dynamic light scattering (DLS) measurements have been done, and the data are shown in Table 3. DLS data show that the histones exist as aggregates in solutions as the individual size of histone molecules is very small. The table shows that the CTAB micellar size is considerably smaller (4 nm radius) than that of the histone H4 cluster (34 nm). The hydrodynamic radius of both the histone-bound and the CTAB-bound ds-DNA complexes are quite similar to each other ($\sim$96 nm) in contrast to the significant difference seen in their longer correlation times, which represent global tumbling dynamics and, hence, the size (Table 2). This apparent anomaly can be understood when we note that DLS measurements are biased by the presence of large particles (due to scattering intensity being proportional to the sixth power of particle size), whereas the rotational dynamics gives a weighted average of the entire population.

Both the fluorescence anisotropy and the DLS measurements show that the stochiometry of binding is not 1:1 with both of the binders. One could model the complexes as large aggregates in which the histone clusters/CTAB micelles are linked by the DNA. The interaction of DNA with histones and CTAB is mainly electrostatic (with an influence of hydrophobic interactions), and the reasons for different affinities of two models could have a contribution from different charge and size parameters and also their clustering tendency. CTAB micelles are in rapid equilibrium with the monomers. The micelles continuously break and reform since the affinity between DNA

TABLE 4: Bimolecular Quenching Constants for ds- and ss-DNA in Free and Bound State[a]

sample ds-DNA	k_q (10^9) (M^{-1} s^{-1})	sample ss-DNA	k_q (10^9) (M^{-1} s^{-1})
A30(1)T30	2.17	A30(1)	2.49
A30(2)T30	2.29	A30(2)	0.67
A30(15)T30	1.46	A30(15)	0.35
A30(1)T30 + H4 histones	0.82	A30(1) + H4 histones	0.40
A30(2)T30 + H4 histones	0.67	A30(2) + H4 histones	0.29
A30(15)T30 + H4 histones	0.73	A30(15) + H4 histones	0.27
A30(1)T30 + CTAB micelles	0.51	A30(1) + CTAB micelles	0.87
A30(2)T30 + CTAB micelles	0.33	A30(2) + CTAB micelles	0.57
A30(15)T30 + CTAB micelles	0.84	A30(15) + CTAB micelles	0.57

[a] Note that the error in the estimation of k_q is 10−15%.

TABLE 5: Parameters Associated with Fluorescence Intensity Decay and Fluorescence Anisotropy Decay in ss-DNA in the Presence of Histone H4 and CTAB Micelles[a]

	fluorescence lifetime (ns) (amplitude)			mean lifetime (ns)	% inc. in	rotational correlation time (ns) (amplitude)	
sample	τ_1 (α_1)	τ_2 (α_2)	τ_3 (α_3)	τ_m	τ_m	ϕ_1 (β_1)	ϕ_2 (β_2)
A30(1)	0.42 (0.30)	1.5 (0.52)	4.1 (0.18)	1.62		0.15 (0.51)	1.1 (0.49)
A30(2)	0.72 (0.27)	1.8 (0.60)	5.9 (0.13)	2.01		0.28 (0.44)	2.1 (0.56)
A30(15)	0.85 (0.25)	2.5 (0.62)	5.4 (0.13)	2.46		0.23 (0.40)	3.5 (0.60)
A30(1) + H4	0.72 (0.38)	2.8 (0.44)	7.8 (0.18)	2.93	81	0.75 (0.37)	26 ± 5 (0.63)
A30(2) + H4	0.53 (0.26)	2.1 (0.45)	6.7 (0.29)	3.06	52	0.81 (0.25)	28 ± 7 (0.75)
A30(15) + H4	0.62 (0.24)	2.4 (0.46)	6.9 (0.30)	3.34	36	0.96 (0.20)	35 ± 10 (0.80)
A30(1) + CTAB	0.67 (0.29)	2.2 (0.49)	4.8 (0.22)	2.36	46	0.43 (0.53)	3.7 (0.47)
A30(2) + CTAB	0.59 (0.26)	2.2 (0.47)	5.9 (0.27)	2.79	39	0.94 (0.42)	12.2 (0.58)
A30(15) + CTAB	0.74 (0.24)	2.6 (0.49)	7.0 (0.27)	3.36	36	1.23 (0.34)	15 (0.66)

[a] Note that the error associated with the estimation of τ_1 is ∼20%, and those of τ_2 and τ_3 are ∼10%, whereas the error in τ_m estimation is ∼5%. The significantly lower value of error associated with τ_m is due to compensation of the larger uncertainties associated with the individual components. The error in ϕ_1 estimation is ∼20%, and that with ϕ_2 is ∼15% unless otherwise stated. Individual values of errors are not given to reduce the clutter.

and CTAB is known to be weak.[70] On the other hand, histones tend to bind DNA more stably due to their interaction with the major groove surface of ds-DNA, whereas CTAB micelles that are bigger in size cannot fit into the grooves. The preference of histones toward the major grooves of ds-DNA has been reported using spermidines and histones in the presence of DNA, whereas the surfactants are known to bind to the ds-DNA at the location of their minor grooves.[25,64]

3.1.3. Fluorescence Quenching Studies. The effect of binding to histones and CTAB micelles on solvent accessibility of different positions of ds-DNA is studied by fluorescence quenching by acrylamide. The value of bimolecular quenching constant k_q is obtained from the SV plots for samples with 2-AP located at varying positions of free and bound ds-DNA. The k_q value is a measure of the degree of solvent exposure of the probe. The values of k_q (Table 4, column 2) are similar for probes at the 1st and 2nd positions but higher than the middle (15th) position, suggesting that the middle position of ds-DNA is the least exposed to the solvent than the end position, probably due to stronger stacking interactions. The value of the quenching constant, k_q, decreases for all of the positions of ds-DNA on binding to the histone and CTAB, showing an overall decrease in the solvent accessibility of the bases caused by the binding. In general, the histone-bound ds-DNA does not show any trend in k_q values with the location of the probe. However, CTAB-bound DNA showed position dependence of k_q. This difference might have originated from the difference in the modes of binding to the histone and CTAB.

3.2. Interaction of ss-DNA (ss-A30) with Histones and CTAB Micelles. It is of interest to check whether the site-specific modulation of dynamics of ds-DNA on binding to either H4 histone or CTAB micelles is also seen with ss-DNA and also to see whether the binding agents can discriminate between ss-DNA and ds-DNA. With these aims, we carried out studies with ss-DNA, A30.

3.2.1. Fluorescence Lifetime Analysis. The fluorescence decay curves of 2-AP located in ss-A30 DNA bound to H4 histones and CTAB micelles have been satisfactorily fitted to the sum of three exponentials (Table 5), unlike the case with ds-DNA, which required a sum of four exponentials. The mean lifetime (τ_m) of the probe increases substantially, irrespective of its location on ss-DNA, on binding to either H4 histone or CTAB micelles. The increase in fluorescence intensity and mean lifetime of ss-DNA, on binding, indicates the expected decrease in flexibility of the bases. The percentage increase in the τ_m value on binding to H4 histones (Table 5, column 7) is higher for 2-AP loacted at the end (∼81%) than at the middle position (∼36%). The τ_m value shows an increasing trend from the end to the middle position of the probe on the bound ss-DNA strand. The ends of the histone-bound ss-DNA show a minimum τ_m value (∼2.9 ns), which emanates from faster internal motion and minimum stacking interaction of the probe at the ends as compared to the middle position that shows a maximum τ_m value (∼3.3 ns). The site-specific differences in lifetime values in the bound ss-DNA suggest that even though ss-DNA is expected to coil around the histone molecules completely, the ends experience more flexibility as compared to the second and middle positions.

3.2.2. Time-Resolved Fluorescence Anisotropy. Figure 2 shows the anisotropy decay traces for probe located at end and middle positions of ss-DNA with and without the binding agents. The values of ϕ_1 and ϕ_2 increase significantly on binding to H4 histone and CTAB micelles, suggesting that binding to the surfaces slows down the motional dynamics of the ss-DNA strand, making the whole strand rigid. A slightly increasing trend is observed in the value of ϕ_1 when the position of 2-AP changes

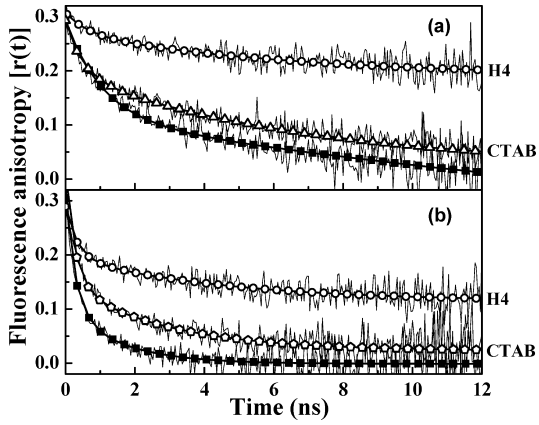

Figure 2. Time-resolved fluorescence anisotropy of 2-AP located in A30 ss-DNA at (a) position 15 and (b) position 1, in free form and condensed form with core histone H4 and CTAB micelles. Filled squares, control; diamonds, CTAB; and open square, H4 histone.

from the end to the middle on histone-bound ss-DNA, indicating fast internal dynamics of bases at the ends that becomes slower toward the middle position of the strands. A higher value of ϕ_2 at the middle position suggests a larger contribution of global tumbling of the entire ss-DNA−histone complex to the overall dynamics as compared to the ends where the ϕ_2 value has more contribution from segmental motion of the strands. One interesting observation is that the ends remain more flexible than the middle position of bound ss-DNA. Once again, this indicates that although binding results in enhanced rigidity of DNA, the internal dynamics of bases are largely preserved and thus ensure the function of DNA in the bound form. This inference can be extended to understand why DNA in chromatin retains its functional ability even while it coils around histones.

DLS measurements show that the hydrodynamic radius of ss-DNA bound to either H4 or CTAB is quite high and that the CTAB complex shows a slightly higher value when compared to the H4 complex (Table 3). However, this trend is opposite to that observed from the long rotational correlation time seen with the samples having 2-AP at position 15 (Table 5). As mentioned earlier, size estimations by DLS and rotational correlation time need not agree with each other, as the former is heavily biased by larger particles and the latter gives a weighted average of the entire population, resulting in a higher apparent value of the size from DLS measurements. Furthermore, the longer rotational correlation time is likely to arise from a combination of segmental and resulting global dynamics; hence, this correlation time may not truly reflect the overall size.

Estimation of the size of the complex by DLS brings out another interesting fact. While the complexes of ss-DNA and ds-DNA with CTAB have similar and large sizes (88 and 94 nm, respectively, Table 3), binding with H4 results in complexes of significantly varying sizes (56 and 98 nm with ss- and ds-DNA, respectively, Table 3). This observation indicates that H4 is able to discriminate between ss- and ds-DNA by its mode of binding, an observation that is consistent with H4 being a known binder of dsDNA in a nucleosomal particle. In contrast, CTAB is unable to offer this discrimination. Thus, we infer that binding of DNA with the histone is more than just an electrostatic interaction as with CTAB micelles. The higher binding capacity of the histone molecules to a duplex when compared to ss-DNA is likely to be due to binding of histone molecules in the major grooves of the ds-DNA strands.[25,64]

3.2.3. Fluorescence Quenching Studies. Quenching of fluorescence by acrylamide has been carried out to see the effect of binding to the histone and CTAB micelles on the extent of solvent exposure of bases in ss-DNA. First, the value of the bimolecular quenching constant k_q decreases significantly when bound to either the histone or the CTAB, reflecting protection of bases from the solvent on binding (Table 4). Second, the level of protection is higher with the histones when compared to CTAB (Table 4). Third, the position dependence of k_q seen in free ss-DNA is maintained in both of the bound forms, indicating that binding does not alter the relative position-dependent dynamics, a conclusion similar to that drawn from fluorescence anisotropy decay studies (see above).

It is interesting to note that the value of k_q for positions 2 and 15 is significantly lower for the free ss-DNA when compared to the free ds-DNA (Table 4). This could be understood on the basis of globular conformation of small ss-DNA fragments. The persistent length of a ss-DNA strand is ∼1 nm; thus, a strand of 30 bps (∼126 Å long considering a ∼4.2 Å rise with each base pair) prefers to exist as globule, resulting in the burial of middle positions, leading to reduced exposure to the solvent and keeping the ends flexible and exposed. An alternate explanation could be the following: The observed k_q could mainly originate from the most fluorescent conformation in both the ss- and the ds-DNA. Because the fractional contribution of this conformation (represented by the longest lifetime value and its amplitude, Tables 2 and 5) varies in the two forms of DNA, the estimated value of k_q could have a contribution from this source also apart from changes in the level of the overall solvent exposure.

4. Conclusions

Site-specific differences in the fluorescence lifetime and anisotropy of 2-AP located at various positions in ds- and ss-DNA have been studied in the presence of H4 histone and CTAB micelles as binding agents. As expected, the flexibility of all positions of DNA is reduced, but more significantly, the fraying motion of the end position is greatly affected. The lifetime of the probe increases on binding to the external binding agents (histones andCTAB micelles), irrespective of its position on ds- and ss-DNA strand. This could be due to cumulative effects of freezing of internal dynamics, changes in base-stacking interactions, and decreases in solvent exposure. On binding to the external agents, stacking interactions in ds-DNA become weak, and the concerted motion of the bases seen in free ds-DNA gets dampened in the bound fomrs. Overall, the dynamics of the bound DNA becomes slow. Histones bind to ds-DNA in the form of clusters and have a more drastic effect on the structure and dynamics of DNA than CTAB micelles. Histones have better binding affinities, as they have the tendency to sit inside the major grooves of the ds-DNA, which is not possible in the case of larger-sized CTAB micelles. Binding of CTAB micelles to DNA is largely nonspecific, while that of histones is more specific as they can discriminate between ss-DNA and ds-DNA while binding.

The comparison between histones and CTAB has provided information about general aspects of site-specific dynamics of both ds- and ss-DNA in the presence of external binding agents. Because of binding, the exposure of bases decreases toward the solvent, which explains how binding agents protect DNA from nucleases, etc. Binding does not dampen the internal dynamics completely and does not compromise the structural integrity of the DNA; thus, the functionality of DNA in chromatin is retained. However, stacking and probably base pairing weaken on binding, which is a hidden boon for the process of transcription. The aspect of base-pair weakening is perhaps an

important physical consequence of bound DNA, which has significant biological implications, including that of "unwinding" the duplex DNA, leading to negative supercoiling. Essentially, all DNA transactions in the genome during transcription/replication/repair involve strand opening that requires base-pair weakening. Even in prokaryotic cells that have no well-defined chromatin-bound DNA, the cellular genome is largely bound to histonelike proteins that induce DNA compaction.[65,66] It is tempting to speculate that perhaps a bound DNA (to histone or histonelike proteins) state that facilitates a base-pair weakening effect must have induced a strong selective pressure in shaping the DNA strand-opening dynamics during various functional transactions in DNA genomes. Although there have been many unanswered issues left in DNA−protein and DNA−surfactant interactions, we believe that even a minimal amount of information in this direction is worth its efforts, given the physical complexity of the genome in the nuclear compartment where local concentrations of binding sites[67] and viscoelastic properties of the interacting systems[68] contribute to functional dynamics,[69] perhaps via the effects described here. We believe that the next step of our study must involve analyses of bound DNA in nucleosomal particles, a step closer to physiological conditions.

Acknowledgment. We thank Prof. N. Periasamy for providing us the software used in the analysis.

References and Notes

(1) Arents, G.; Moudrianakis, E. N. *Proc. Natl. Acad. Sci. U.S.A.* **1993**, *90*, 10489–10493.
(2) Cairns, B. R. *Nature* **2009**, *461*, 193–198.
(3) El Aneed, A. *J. Controlled Release* **2004**, *94*, 1–14.
(4) Goula, D.; Benoist, C.; Mantero, S.; Merlo, S.; Levi, G.; Demeneix, B. A. *Gene Ther.* **1998**, *5*, 1291–1295.
(5) Shilatifard, A. *Annu. Rev. Biochem.* **2006**, *75*, 243–269.
(6) Eldridge, A. M.; Halsey, W. A.; Wuttke, D. S. *Biochemistry* **2006**, *45*, 871–879.
(7) Chubb, J. R.; Boyle, S.; Perry, P.; Bickmore, W. A. *Curr. Biol.* **2002**, *12*, 439–445.
(8) Tarahovsky, Y. S.; Rakhmanova, V. A.; Epand, R. M.; MacDonald, R. C. *Biophys. J.* **2002**, *82*, 264–273.
(9) Miller, A. D. *Angew. Chem., Int. Ed.* **1998**, *37*, 1768–1785.
(10) Krishnamoorthy, G.; Duportail, G.; Mely, Y. *Biochemistry* **2002**, *41*, 15277–15287.
(11) Mel'nikov, S. M.; Sergeyev, V. G.; Melnikova, Y. S.; Yoshikawa, K. *J. Chem. Soc. (Faraday Trans.)* **1997**, *93*, 283–288.
(12) Krishnamoorthy, G.; Roques, B.; Darlix, J.-L.; Mely, Y. *Nucleic Acids Res.* **2003**, *31*, 5425–5432.
(13) Nelson, D. L.; Cox, M. M. *Lehninger, Principles of Biochemistry*, 4th ed.; W. H. Freeman & Company: New York, 2004.
(14) Jenuwein, T.; Allis, C. D. *Science* **2001**, *293*, 1074–1080.
(15) Moret, I.; Peris, J. E.; Guillem, V. M.; Benet, M.; Revert, F.; Dasi, F.; Crespo, A.; Alino, J. *J. Controlled Release* **2001**, *76*, 169–181.
(16) Tarahovsky, Y. S.; Rakhmanova, V. A.; Epand, R. M.; MacDonald, R. C. *Biophys. J.* **2002**, *82*, 264–273.
(17) Weintraub, H. *Cell* **1985**, *42*, 705–711.
(18) Kalyansundaram, K. *Photochemistry in Microheterogeneous Systems*; Academic Press: Orlando, FL, 1987.
(19) Dias, R. S.; Lindman, B.; Miguel, M. G. *J. Phys. Chem. B* **2002**, *106*, 12600–12607.
(20) Cardenas, M.; Braem, A.; Nylander, T.; Lindman, B. *Langmuir* **2003**, *19*, 7712–7718.
(21) Bonincontro, A.; Marchetti, S.; Onori, G.; Rosati, A. *Chem. Phys.* **2005**, *312*, 55–60.
(22) Spink, C. H.; Chaires, J. B. *J. Am. Chem. Soc.* **1997**, *119*, 10920–10928.
(23) Jadhav, V. M.; Valaske, R.; Maiti, S. *J. Phys. Chem. B* **2008**, *112*, 8824–8831.
(24) Behr, J. P.; Demeneix, B.; Loeffler, J. P.; Perez-Mutul, J. *Proc. Natl. Acad. Sci. U.S.A.* **1989**, *86*, 6982–6986.
(25) Pattarkine, M. V.; Ganesh, K. N. *Biochem. Biophys. Res. Commun.* **1999**, *263*, 41–46.
(26) Genest, D.; Wahl, P.; Erard, M.; Champagne, M.; Daune, M. *Biochimie* **1982**, *64*, 419–427.
(27) Genest, D.; Sabeur, G.; Wahl, P.; Auchet, J. C. *Biophys. Chem.* **1981**, *13*, 77–87.
(28) Wang, J.; Hogan, M.; Austin, R. H. *Proc. Natl. Acad. Sci. U.S.A.* **1982**, *79*, 5896–5900.
(29) Ashikawa, I.; Kinosita, K.; Ikegami, A.; Nishimura, Y.; Tsuboi, M.; Watanabe, K.; Iso, K. *J. Biochem.* **1983**, *93*, 665–668.
(30) Winzeler, E. A.; Small, E. W. *Biochemistry* **1991**, *30*, 5304–5313.
(31) Brown, D. W.; Libertini, L. J.; Small, E. W. *Biochemistry* **1991**, *30*, 5293–5303.
(32) Pedone, F.; Mazzei, F.; Santoni, D. *Biophys. Chem.* **2004**, *112*, 77–88.
(33) Dubertret, B.; Liu, S.; Ouyang, Q.; Libchaber, A. *Phys. Rev. Lett.* **2001**, *86*, 6022–6025.
(34) Shih, C. C.; Georghiou, S. *Biopolymers* **2006**, *81*, 450–463.
(35) Olson, W. K.; Zhurkin, V. B. *Curr. Opin. Struct. Biol.* **2000**, *10*, 286–297.
(36) Rai, P.; Cole, T. D.; Thompson, E.; Millar, D. P.; Linn, S. *Nucleic Acids Res.* **2003**, *31*, 2323–2332.
(37) Cheatham, T. E. *Curr. Opin. Struct. Biol.* **2004**, *14*, 360–367.
(38) Zhang, Q.; Sun, X.; Watt, E. D.; Al-Hashim, H. M. *Science* **2006**, *311*, 653–656.
(39) Jean, J. M.; Hall, K. B. *Biochemistry* **2002**, *41*, 13152–13161.
(40) Rachofsky, E. L.; Osman, R.; Ross, J. B. A. *Biochemistry* **2001**, *40*, 946–956.
(41) Jean, J. M.; Hall, K. B. *Proc. Natl. Acad. Sci. U.S.A.* **2001**, *98*, 37–41.
(42) Holmein, A.; Norden, B.; Albinsson, B. *J. Am. Chem. Soc.* **1997**, *119*, 3114–3121.
(43) Bandwar, R. P.; Patel, S. S. *J. Biol. Chem.* **2001**, *276*, 14075–14082.
(44) Guest, C. R.; Hochstrasser, R. A.; Sowers, L. C.; Millar, D. P. *Biochemistry* **1991**, *30*, 3271–3279.
(45) Ramreddy, T.; Rao, B. J.; Krishnamoorthy, G. *J. Phys. Chem. B* **2007**, *111*, 5757–5766.
(46) Ramreddy, T.; Sen, S.; Rao, B. J.; Krishnamoorthy, G. *Biochemistry* **2003**, *41*, 12085–12094.
(47) Lakowicz, J. R. *Principles of Fluorescence Spectroscopy*, 3rd ed.; Springer: New York, 2006.
(48) Lakshmikanth, G. S.; Krishnamoorthy, G. *Biophys. J.* **1999**, *77*, 1100–1106.
(49) Swaminathan, R.; Nath, U.; Udgaonkar, J. B.; Periswami, N.; Krishnamoorthy, G. *Biochemistry* **1996**, *28*, 9150–9157.
(50) Saxena, A. M.; Udgaonkar, J. B.; Krishnamoorthy, G. *J. Mol. Bio.* **2006**, *359*, 174–189.
(51) Mukhopadhyay, S.; Nayak, P. K.; Udgaonkar, J. B.; Krishnamoorthy, G. *J. Mol. Biol.* **2006**, *358*, 935–942.
(52) Karthikeyan, G.; Wagle, M. D.; Rao, B. J. *FEBS Lett.* **1998**, *425*, 45–51.
(53) Sen, S.; Karthikeyan, G.; Rao, B. J. *Biochemistry* **2000**, *33*, 10196–10206.
(54) Sen, S.; Krishnamoorthy, G.; Rao, B. J. *FEBS Lett.* **2001**, *491*, 289–298.
(55) Navadgi, V. M.; Sen, S.; Rao, B. J. *Biochem. Biophys. Res. Commun.* **2002**, *296*, 983–987.
(56) Ramreddy, T.; Kombrabail, M.; Krishnamoorthy, G.; Rao, B. J. *J. Phys. Chem. B* **2009**, *113*, 6840–6846.
(57) O'Connor, D. V.; Phillips, D. *Time Correlated Single Photon Counting*; Academic Press: London, 1984; pp 180−189.
(58) Bevington, P. R. *Data Reduction and Error Analysis for the Physical Sciences*; McGraw-Hill, Inc.: New York, 1969.
(59) Nag, N.; Rao, B. J.; Krishnamoorthy, G. *J. Mol. Biol.* **2007**, *374*, 39–53.
(60) Larsen, O. F.; van Stokkum, I. H.; Gobets, B.; van Grondelle, R.; van Amerongen, H. *Biophys. J.* **2001**, *81*, 1115–1126.
(61) Hochstrasser, R. A.; Carver, T. E.; Sowers, L. C.; Millar, D. P. *Biochemistry* **1994**, *39*, 11971–11979.
(62) Kodali, G.; Kistler, K. A.; Matsika, S.; Stanley, R. J. *J. Phys. Chem. B* **2008**, *112*, 1789–1795.
(63) Georghiou, S.; Bradrick, T. D.; Philippetis, A.; Beechem, J. M. *Biophys. J.* **1996**, *70*, 1909–1922.
(64) Berr, S. S.; Jones, R. R. M. *Langmuir* **1988**, *4*, 1247–1251.
(65) Dame, R. T. *Mol. Microbiol.* **2005**, *56*, 858–870.
(66) Stavans, J.; Oppenheim, A. *Phys. Biol.* **2006**, *3*, R1–R10.
(67) Grünwald, D.; Martin, R. M.; Buschmann, V.; Bazett-Jones, D. P.; Leonhardt, H.; Kubitscheck, U.; Cardoso, M. C. *Biophys. J.* **2008**, *94*, 2847–2858.
(68) Iborra, F. J. *Theor. Biol. Med. Model.* **2007**, *4*, 15.
(69) Lamond, A. I.; Spector, D. L. *Nat. Rev. Mol. Cell Biol.* **2003**, *4*, 605–612.
(70) Llere, D.; Clamme, J.-P.; Dauty, E.; Blessing, T.; Krishnamoorthy, G.; Duportail, G.; Mely, Y. *Langmuir* **2002**, *18*, 10340–10347.

JP912029M